JOURNAL OF PROPULSION AND POWER
Vol. 20, No. 6, November–December 2004

Decomposition of Hydrogen Peroxide on MnO_2/TiO_2 Catalysts

Annamaria Russo Sorge,* Maria Turco,† Giuseppe Pilone,‡ and Giovanni Bagnasco§
University of Naples, "Federico II," 80125 Naples, Italy

Catalysts containing 2–10 wt% MnO_2 supported on TiO_2 were examined for H_2O_2 decomposition. Catalysts were prepared by impregnation of a high TiO_2 surface area. X-ray defraction patterns, scanning electron micrographs, and surface area measurements gave evidence of a uniform distribution of the active phase on the support surface and of the absence of segregated manganese oxides phases. Temperature programmed reduction measurements showed the presence, beside MnO_2, of different Mn oxides species formed by interaction between the active phase and the support surface. The MnO_2 reducibility increased, whereas the mean oxidation state of manganese decreased with increasing manganese content. Catalytic tests were performed in a batch reactor with 50 or 70% concentration H_2O_2 solutions. Catalytic activity was very high at the beginning of the tests and decreased with time, reaching a final constant value that increased with manganese content. Kinetic constants, evaluated assuming a first-order reaction rate, were comparable or higher than those of similar manganese-based catalysts. An optimal MnO_2 content was found, corresponding to the quite complete surface monolayer coverage. A reaction mechanism involving an Mn^{4+}–Mn^{3+} redox couple has been proposed.

Nomenclature

H	=	enthalpy, J
k	=	kinetic constant (volumic), s^{-1} cm^3_{sol} $(cm^3_{cat})^{-1}$
k'	=	kinetic constant (molar), s^{-1} cm^3_{sol} $(mol_{MnO2})^{-1}$
n	=	mol H_2O_2
n_0	=	initial mol H_2O_2
T	=	temperature, °C
t	=	time, h
V_{cat}	=	volume of catalyst, cm^3
V_{sol}	=	volume of H_2O_2 solution, cm^3

Introduction

THE concept of low-cost access to space and the increasing number of space vehicles impose the necessity to research new propellants and new propulsion mechanisms to satisfy requirements of safety, low cost, and over all environment friendliness, now considered of primary importance. Several mission criteria such as a spacecraft's attitude control, orbital maneuvers, orbit injection of satellites, crew rescue vehicles from the International Space Station (ISS) all require the named these necessities, as well as a stop-to-restart capability. Hydrogen peroxide has been investigated in recent years as an alternative propellant to the most widely employed propellants, such as hydrazine or nitrogen tetroxide/monomethylhydrazine (NTO/MMH) because of the advantages of low toxicity and low environmental impact and because its decomposition produces no pollutant species.[1–4] Moreover, hydrogen peroxide satisfies other technical requirements such as long-term stability and the possibility of starting its decomposition without any ignition device. This last property can be achieved by the use of highly concentrated hydrogen peroxide, known as high-test hydrogen peroxide (HTP). It is most significant because it allows for restart capability without an excessive increase in weight and complexity of the motor structure.

Received 16 May 2003; revision received 27 February 2004; accepted for publication 5 March 2004.

*Associate Professor, Department of Space Science and Engineering; russosor@unina.it. Member AIAA.
†Associate Professor, Department of Chemical Engineering; turco@unina.it.
‡Undergraduate Student, Department of Space Science and Engineering.
§Researcher, Department of Chemical Engineering.

Hydrogen peroxide decomposition,

$$2H_2O_{2(l)} \rightarrow 2H_2O_{(g)} + O_{2(g)}, \qquad \Delta H = -94{,}355\,\mathrm{J\ mol^{-1}} \quad (1)$$

has no thermodynamic limitations and, when performed in adiabatic conditions, can produce hot gases at $T = 613$–996°C, depending on the H_2O_2 concentration (85–100%). Resultant gases can be directly expanded in a nozzle (monopropellant configuration) or injected in a combustion chamber to prime the combustion with a solid or liquid propellant (bipropellant configuration). The decomposition rate of practical appliances can be obtained only in the presence of suitable catalysts. The catalyst properties and the catalytic reactor design are fundamental aspects for the development of propulsive systems using HTP. A suitable catalyst must exhibit high activity in a wide range of operating conditions (varying from H_2O_2 liquid phase at room temperature to H_2O_2 vapor phase up to the adiabatic decomposition temperature), from structural and chemical stability for a long operating life with frequent ignition/shut down cycles to high resistance to thermal and mechanical shocks. Moreover, high resistance to stabilizing agents (phosphates, stannates, nitrates) normally added to HTP solutions to improve its long-term stability is also an important feature. The catalytic bed must also guarantee very short response times (<100 ms) to obtain a reliable attitude control. Low pressure drops and limited weight are also required. Catalytic reactors generally contain packed beds made of silver-electroplated stainless-steel screens. However, these reactors show some disadvantages, such as large pressure drops, high weight, and deactivation due to the stabilizers.[5] Hence, there is an interest in the development of new catalytic systems.

Recent literature points to manganese-based catalysts as the most promising alternative to metallic catalysts.[6] Pure, mixed, or supported manganese oxides were largely investigated. Among different MnO_x compounds, MnO_2, Mn_3O_4, Mn_5O_8 exhibited high activity, whereas Mn_2O_3 was found to be completely inactive.[7] The activity of some MnO_x phases, such as β-MnO_2, colloidal MnO_2, or Mn_3O_4, was related to the presence in reaction conditions of different Mn oxidation states and to high electronic mobility.[7–9] Several mixed oxides containing Mn and either another transition metal[6,7,10–12] or lead[13] or bismuth[7] were investigated for H_2O_2 decomposition. Generally, mixed oxides were found to be more active than pure MnO_x systems, due to the presence of metal ions with different charges on the catalyst surface.[7] Moreover, manganese oxides alkalized with addition of group 1 or 2 metals, such as K or Ba, showed improved catalytic activity due to a higher electron density and the mobility of surface oxygen.[8] Interesting results were also obtained with manganese oxide octahedral molecular sieves (OMS) containing Mg^{2+} or first row transition metal ions such as

Ni^{2+}, Cu^{2+}, Co^{2+}, and Fe^{3+} (Ref. 10). Some recent works deal with manganese-based perovskites derived from $LaMnO_3$ or $NdMnO_3$ by partial substitution of Sr or K for La or Nd (Refs. 14 and 15). Similar alumina-supported perovskites were studied for monopropellant thrusters.[16] The activity of Mn perovskites was related to Mn^{4+} cations[14] or to oxygen vacancies.[15]

Many researchers studied H_2O_2 decomposition on Mn oxides supported on different materials, such as SiO_2 (Ref. 12), Al_2O_3 (Refs. 6 and 17–21), SiO_2–Al_2O_3 (Ref. 6), ZrO_2 (Ref. 22), zeolites (Ref. 6) or monolithic cordierite substrates.[23] The results of these studies suggest that catalytic properties of Mn oxides are markedly influenced by the type of support, hence, the interest in new, supported catalysts containing high concentrations of surface active species that can be stable under reaction conditions. Manganese oxides supported on TiO_2 were widely studied for catalytic processes,[24–26] but they have received no attention for H_2O_2 decomposition. These catalysts could be interesting for the high surface area and the strong interaction between MnO_2 and TiO_2 that can stabilize the oxidation state Mn^{4+}.

In this work, catalysts based on MnO_2 supported on high surface area TiO_2 were studied for the decomposition of hydrogen peroxide. Chemical and physical characterizations were also performed to obtain information on the surface chemical properties involved in catalytic reaction.

Tests Facility and Experimental Activity

Catalysts Preparation

MnO_2/TiO_2 catalysts were prepared by impregnation of high surface area TiO_2 (anatase phase, with traces of brookite phase) supplied by Tioxide (120 m^2g^{-1}) with $Mn(CH_3COO)_2 \times 4H_2O$ solutions. All of the materials were dried at 120°C and calcined at 500°C in airflow. Nominal MnO_2 contents were 2, 5, 7, and 10 wt%. The materials are listed according to the nominal MnO_2 content, as reported in Table 1. Commercial Mn_2O_3 and MnO_2 were supplied by Carlo Erba, Milan, Italy (R.P. products).

Physical and Chemical Characterization

X-ray diffraction patterns (XRD) were obtained by the use of a Philips diffractometer PW 1100 apparatus. Scanning electron micrographs (SEM) and elemental analysis by an electronic display system (EDS) technique were affected with a Philips XL 30 instrument. The resolution of compositional analysis is about 1 μm. Specific surface area measurements [Brunauer, Emmett, Teller (BET) method] were performed by N_2 adsorption at 77 K by the use of a Carlo Erba Sorptomatic 1900 (accuracy ± 3 m^2g^{-1}). Temperature programmed reduction (TPR) tests were effected with a Micromeritics 2900 apparatus.

Catalytic Activity Measurements

Catalytic activity measurements were performed by means of the laboratory apparatus shown in Fig. 1. The batch reactor was a flask of volume $V = 200\,cm^3$ thermostated by an electronically controlled water bath. The catalyst powder (weight = 25–150 $\pm$ 0.1 mg, grain dimensions = 71–150 μm, apparent density = $1 \pm 0.1\ g \cdot cm^{-3}$) was maintained in suspension in the H_2O_2 solution ($V_{sol} = 100 \pm 1\ cm^3$) by stirring.

H_2O_2 solutions were supplied by Sigma–Aldrich (50%) and Degussa AG (70%) without information about the concentration

Table 1 MnO_2 content and specific surface area of Mn/Ti catalysts

Sample	MnO_2[a]	wt%[b]	Surface area, m^2g^{-1}
TiO_2	——	——	129
2-Mn/Ti	2	2.7	106
5-Mn/Ti	5	5.3	93
7-Mn/Ti	7	7.3	88
10-Mn/Ti	10	11.0	85
MnO_2	——	——	53
Mn_2O_3	——	——	30

[a]Nominal contents. [b]From EDS analysis.

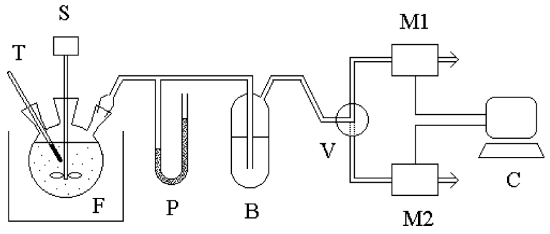

Fig. 1 Apparatus for catalytic activity measurements: F, flask; T, thermometer; S, stirrer; P, pressure gauge; B, bubbler; V, three-way valve; M1 and M2, flow meters; and C, computer.

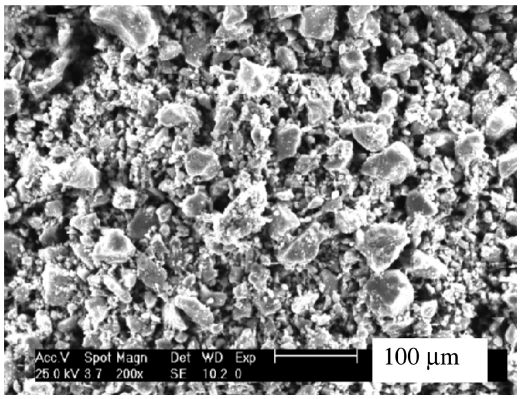

Fig. 2 SEM of 10-Mn/Ti sample (low magnification).

of the stabilizers. The rate of oxygen production was continuously measured by mass flow meters. Two mass flow meters of different flow ranges (10 $dm^3\ h^{-1}$ and 100 $dm^3\ h^{-1}$) could be selected. The accuracy of flow rate measurements was $\pm$3%. This method, unlike other ones (volumetric, titrimetric, refractometric, etc.), allows direct measurement of the reaction rate, without any derivative operation. A trap was inserted at the outlet of the reactor to eliminate some fog that could be carried by the oxygen stream. The reaction tests were effected at $T = 40$, 70°C, H_2O_2 concentrations = 50 and 70%, and catalyst volume to solution volume ratios $V_{cat}/V_{sol} = 1.5 \cdot 10^{-4}$–$1.5 \cdot 10^{-3}$.

Results and Discussion

Physical Characterization

In Figs. 2 and 3, SEM of a 10-Mn/Ti catalyst with different magnifications are shown. Note that a satisfactory homogeneity of the sample, which is composed of irregularly shaped particles with dimensions of about 30 μm. A similar morphology is shown by the other samples, which also appear homogeneous.

EDS analysis shows that manganese concentration is constant throughout the surface of the catalysts. This suggests that manganese oxide is not segregated as a distinct phase, but is evenly dispersed on the surface of the support.

The MnO_2 content of samples, evaluated from EDS analysis, is reported in Table 1. We observe that the analyzed values are very close to the nominal contents. When the surface area of the support and the area covered by a MnO_2 unit (15 $Å^2$) (Ref. 25) are taken into account, the MnO_2 content corresponding to the support monolayer coverage is 10.4 wt%. Therefore, the MnO_2 loading of the catalysts corresponds to submonolayer to monolayer support surface covering.

XRD analysis was performed to study the phases composition of the catalysts and also to identify the manganese oxides eventually present as segregate phases. The diffraction patterns obtained on pure TiO_2 and MnO_2 and on Mn/Ti catalysts are reported in Fig. 4. Pure TiO_2 shows the signals of anatase phase, with minor amounts of the brookite phase (signals at $2\Theta = 25.05$ and 31.01 deg; respectively). From the peak width, a mean size of TiO_2 crystals of 120 Å is estimated, corresponding to surface area of 125 m2g-1, in

Table 2 H_2 consumption and temperature of TPR peaks

Sample	T_{max}, °C	H_2 consumption mol g^{-1}	H_2 consumption mol (mol Mn)$^{-1}$	Mean Mn oxidation state
Mn_2O_3	550	0.61×10^{-2}	0.48	3
MnO_2	367, 450	1.06×10^{-2}	0.92	4
2-Mn/Ti	340, 480	2.4×10^{-4}	1.04	4.0
5-Mn/Ti	337	4.9×10^{-4}	0.84	3.7
7-Mn/Ti	348	6.2×10^{-4}	0.80	3.6
10-Mn/Ti	340	8.1×10^{-4}	0.70	3.4

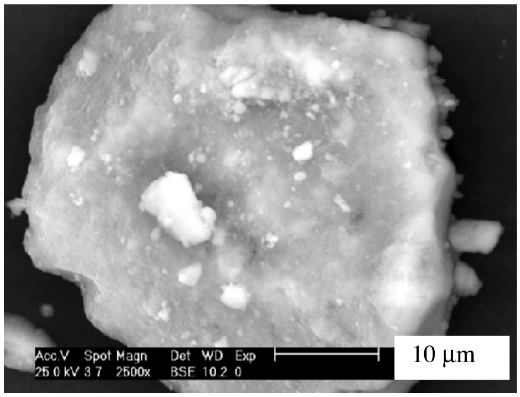

Fig. 3 SEM of 10-Mn/Ti sample (high magnification).

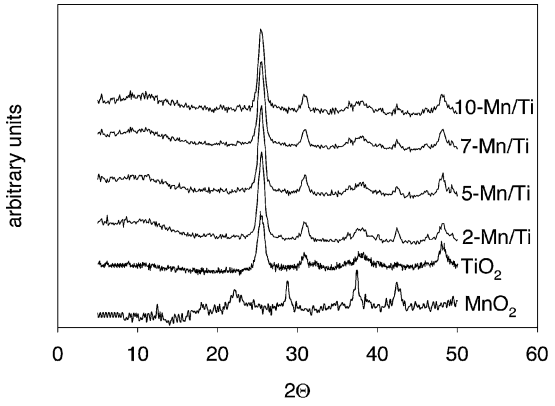

Fig. 4 XRD patterns of MnO_2, TiO_2 and Mn/Ti catalysts.

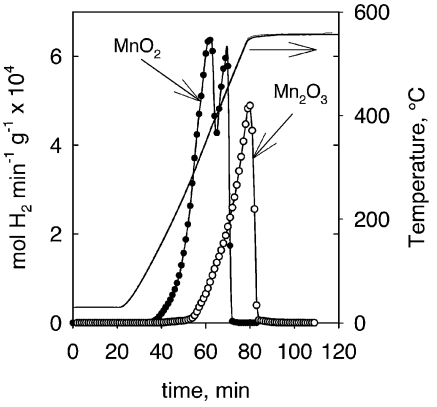

Fig. 5 TPR profiles of MnO_2 and Mn_2O_3.

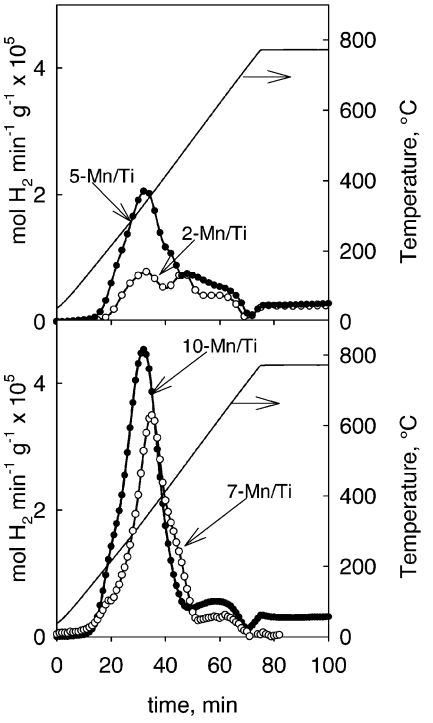

Fig. 6 TPR profiles of Mn/Ti catalysts.

agreement with the BET value (Table 1). All of the catalysts show patterns characteristic of these phases, whereas the signals of manganese oxides phases (MnO, Mn_3O_4, Mn_2O_3, and MnO_2) are absent for all compositions. This result points to a uniform dispersion of the active phase on the surface of the support according to the results of SEM and EDS analysis. Moreover, the characteristic signals of the TiO_2 rutile phase are absent. This indicates that catalysts are thermally stable in the conditions adopted for their preparation. Specific surface areas (Table 1) are lower than that of TiO_2 and gradually decrease with MnO_2 contents. This behavior agrees with a monolayer coverage model, thus, further confirming that the active phase is uniformly dispersed on a TiO_2 surface.

Characterization of Redox Properties

Reference Materials: TiO_2, Mn_2O_3, and MnO_2

TiO_2 support undergoes no reduction in the adopted experimental conditions, as shown by the absence of TPR peaks. TPR profiles of the reference MnO_2 and Mn_2O_3 oxides are reported in Fig. 5. MnO_2 shows two partially overlapped peaks, with a shoulder at about 330°C. The corresponding amount of consumed hydrogen, listed in Table 2, agrees with the reduction to MnO, as already observed.[27] The two peaks in the TPR profile of MnO_2 appear to be of different intensities, the first one corresponding to about 65% of the total amount of consumed H_2. On the basis of the amounts of consumed H_2, we can assume that the first TPR peak corresponds to the reduction $MnO_2 \rightarrow Mn_3O_4$, whereas the second peak corresponds to the reduction $Mn_3O_4 \rightarrow MnO$. When the results by Christel et al.[28] obtained by the ThermoGravimetrical (TG) technique are taken into account, we can assume that reduction of MnO_2 to Mn_3O_4 occurs through two steps: $MnO_2 \rightarrow Mn_2O_3 \rightarrow Mn_3O_4$.

The first reduction step of this sequence can explain the presence of a shoulder on the low TPR peak.

The TPR profile of Mn_2O_3 shows one peak with maximum at ~560°C and agrees with results by Liu et al.[29] although the peak temperature is slightly higher. The amount of consumed H_2 (Table 2) corresponds to reduction to MnO, in agreement with previous studies.[27]

The reduction of Mn_2O_3 to MnO occurs in a temperature range markedly higher than that observed for MnO_2 reduction. Most likely, the reduction of MnO_2 to Mn_2O_3 leads to formation of a poorly crystalline and highly reactive Mn_2O_3 that is more reducible than crystalline Mn_2O_3.

Mn/Ti Catalysts

TPR profiles of Mn/Ti catalysts, shown in Fig. 6, appear more complex than pure oxides. All TPR spectra have their mean peak at low temperature (340–350°C), followed by a high-temperature signal (~600°C). A medium temperature signal (~450°C) is well

evident for the sample 2-Mn/Ti, whereas it appears as a shoulder of the low-temperature peak for samples 5-Mn/Ti and 7-Mn/Ti. It is not observed for the sample 10-Mn/Ti, probably because it overlaps to the low-temperature signal, and the two components become no more distinguishable.

By an increase in the manganese content, the onset temperature decreases and shoulders at 200–220°C appear for the samples with higher Mn content. Similar TPR curves were obtained by Villaseñor et al. for Mn/TiO_2 catalysts, which suggests the presence of two different manganese oxide species.[30] The low shifting of the curve onset and of the medium temperature signal with increasing manganese contents suggests formation of more reducible MnO_2 species with increasing TiO_2 surface coverage. In Table 2, we have reported values of H_2 consumption and of the mean Mn oxidation state, calculated from H_2 consumption. Note that the mean oxidation state of Mn is +4 only in 2-Mn/Ti and decreases with Mn loading. Similar values of Mn oxidation state were found in Ref. 30 for 10% MnO_2 supported on TiO_2 and were related to the presence of some Mn in a +2 or +3 oxidation state. The presence of Mn^{3+} species in MnO_2/TiO_2 catalysts was detected by UV–visible spectra.[25,31] Mn^{2+} species can also be present as a phase $MnTiO_3$ (Ref. 25).

When TPR spectra of pure Mn oxides and results from the are taken into account literature the low-temperature peak can be attributed to the reduction $MnO_2 \rightarrow Mn_3O_4$. The medium temperature signal that shifts to lower temperatures with increasing manganese content can be related to the reduction $Mn_3O_4 \rightarrow MnO$. The low shifting of the curve onset and of the medium-temperature signal with increasing manganese contents suggests formation of more reducible manganese oxide species with increasing TiO_2 surface coverage. The high-temperature signal can be assigned to hardly reducible manganese species. These could be a form of Mn_2O_3 because the peak temperature is close to that of pure Mn_2O_3 (Fig. 5). However, we cannot exclude the contribution of an $Mn_xTi_{1-x}O_2$ solid solution formed by interaction of MnO_2 with TiO_2 (Ref. 25) that should hardly be more reducible than pure MnO_2.

The preceding data point out that redox properties of the active phase are significantly modified by dispersion on TiO_2. To summarize the characterization results, the following manganese oxides species can be hypothesized in the Mn/Ti samples: 1) a form of MnO_2 that is more reducible than crystalline MnO_2, probably due to the high dispersion, or 2) a hardly reducible Mn species, such as Mn_2O_3 or solid solution MnO_2–TiO_2.

Catalytic Activity

Preliminary tests were performed on pure TiO_2 to ascertain the eventual catalytic activity of the support that is partially uncovered in the catalysts with low Mn contents. Catalytic tests were also performed on the pure phases Mn_2O_3 and MnO_2. In all of the investigated experimental conditions, the support and the Mn_2O_3 phase show negligible activity for H_2O_2 decomposition. By contrast, MnO_2 shows high activity, as shown in Fig. 7, where the rate of oxygen production is plotted as a function of time for two different V_{cat}/V_{sol} values. The oxygen flow rates are extremely high at the beginning of the tests, and decrease with time, reaching constant values after about 0.5 h. For this reason, the measurement of evolved oxygen is inaccurate in the first few minutes of the tests. The final constant values, listed in Table 3, are nearly proportional to the amount of catalyst. These tests confirm that Mn^{4+} ions are probably involved in H_2O_2 decomposition. High activity of the MnO_2 phase was also observed by other researchers.[7] However, pure MnO_2 has lower thermal stability than supported catalysts[6] and appears unsuitable for practical applications.

A similar behavior is also observed for Mn/Ti catalysts, as shown in Figs. 8 and 9, which report results obtained at 40°C with 50%

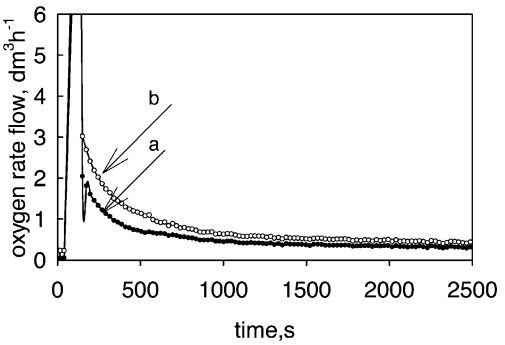

Fig. 7 Oxygen flow rate as a function of time for MnO_2, 50% H_2O_2, and $T = 40°C$: a) $V_{cat}/V_{sol} = 0.15 \times 10^{-3}$ and b) $V_{cat}/V_{sol} = 0.20 \times 10^{-3}$.

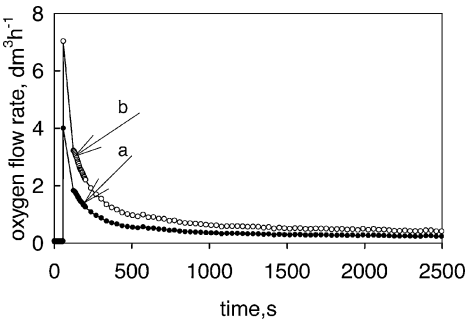

Fig. 8 Oxygen flow rate as a function of time for 7-Mn/Ti catalyst, 50% H_2O_2, and $T = 40°C$: a) $V_{cat}/V_{sol} = 1 \times 10^{-3}$ and b) $V_{cat}/V_{sol} = 1.5 \times 10^{-3}$.

Table 3 Oxygen flow rate and reaction rate in stationary conditions for MnO_2 and Mn/Ti catalysts

$V_{cat}/V_{sol} \times 10^3$	Temperature °C	H_2O_2 concentration wt%	Oxygen flow rate[a] $dm^3 \cdot h^{-1}$	Reaction rate, $mol \cdot s^{-1} \cdot cm^{-3} \times 10^5$
		MnO_2		
0.15	40	50	0.43	67
0.20	40	50	0.60	70
		2-Mn/Ti		
1	40	50	——	——
1	70	50	0.36	8.3
		5-Mn/Ti		
1	40	50	——	——
1	40	70	0.21	4.9
		7-Mn/Ti		
1	40	50	0.34	8.0
1.5	40	50	0.60	9.3
1	40	70	0.53	12.2
		10-Mn/Ti		
1	40	50	0.43	9.9
1.5	40	50	0.62	9.6
1	40	70	0.66	15.3

[a]Measured at $T = 20°C$ and $P = 1$ bar.

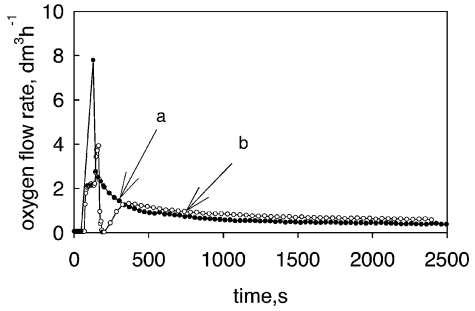

Fig. 9 Oxygen flow rate as a function of time for 10-Mn/Ti catalyst. 50% H_2O_2, and $T = 40°C$: a) $V_{cat}/V_{sol} = 1 \times 10^{-3}$ and b) $V_{cat}/V_{sol} = 1.5 \times 10^{-3}$.

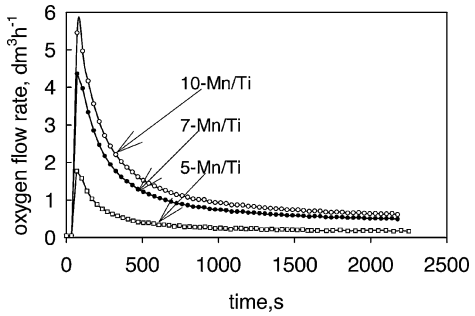

Fig. 10 Oxygen flow rate as a function of time for Mn/Ti catalysts, 70% H_2O_2, $T = 40°C$, and $V_{cat}/V_{sol} = 1 \times 10^{-3}$.

H_2O_2 on catalysts 7-Mn/Ti and 10-Mn/Ti, respectively. The initial rate of oxygen production is always very high, but decreases with time, reaching a stationary value that is largely lower than the initial value after a time of about 0.5 h. The final stationary values of oxygen production (Table 3) are nearly proportional to the amounts of catalysts and appear to increase with Mn content. The catalysts 2-Mn/Ti and 5-Mn/Ti show markedly lower activity, and, after a rapid initial transient, give stationary oxygen production rates that are below the sensitivity limits of the flow meters. A comparison between different catalysts cannot be affected on the basis of initial oxygen evolution rates because the sudden increase of pressure that occurs at the beginning of tests hinders accurate measurements under these conditions.

To investigate on the effect of H_2O_2 concentration on the reaction kinetics, some tests are performed with 70% H_2O_2 solution. The results of tests with 70% H_2O_2 at 40°C are shown in Fig. 10 for different catalyst compositions.

Likewise in these conditions, the 2-Mn/Ti sample shows no appreciable activity. The curves of oxygen evolution as a function of time are similar to those for 50% H_2O_2 tests, with an initial high activity that decreases with time up to a stationary value. As expected, the final values are higher than those observed for the 50% H_2O_2 tests (Table 3) and increase with Mn content.

In all catalytic tests carried out at 40°C, a large temperature increase (10°C) is observed at the beginning of the tests. However, this markedly decreases with time. In the final stationary conditions, it was always lower than 3°C. Therefore, the final values of oxygen evolution rates can give a reliable comparison among the activity of different catalysts.

Measurements of catalytic activity at 70°C are performed with 50% H_2O_2 solutions. Higher reaction rates are observed, and the stationary value is reached in shorter time at 70°C (about 5 min). At this temperature, the 2-Mn/Ti and 5-Mn/Ti catalysts also show an appreciable oxygen production, suggesting a strong activation of the reaction by temperature. However, in these conditions, the high reaction rate leads to a marked increase of reaction temperature during tests with high manganese catalysts. Temperature increases between 7–11°C are measured in stationary conditions and are largely dependent on the catalyst composition. Therefore, a comparison among different catalysts is not significative in these conditions, and only data obtained on the less active 2-Mn/Ti are reported (Table 3). This catalyst, which appeared inactive at 40°C, shows an appreciable oxygen production at 70°C, reaching a stationary value of about 0.36 $dm^3\ h^{-1}$ after a short time.

The decrease of activity during the initial transient time, observed in all catalytic tests, could be due to different effects. The presence of stabilizing components in the H_2O_2 solutions could cause partial poisoning of the catalyst surface, leading to a decrease of the active sites' concentration. This effect should be due mainly to the presence of pyrophosphate ions that can react with manganese oxides, leading to the formation of manganese phosphate or pyrophosphate.[5] However, other hypotheses could be suggested. Under reaction conditions, some MnO_2 reduction could occur, leading to formation of the Mn_2O_3 phase with consequent loss of activity, as previously reported.[7] Moreover, it has been hypothesized that the decrease of activity could be due to the formation and subsequent growth of a film of gaseous oxygen in the catalytsts' pores that hinders the access of the reactant to the inner surface.[7]

Rates of H_2O_2 decomposition referred to by catalyst volume (mole per second per cubic centimeter) are calculated, according to reaction stoichiometry, from oxygen flow rates measured when the final constant values are reached (Table 3).

Data of Table 3 that refer to 7-Mn/Ti and 10-Mn/Ti catalysts show that increasing H_2O_2 concentration from 50% (17.5 $mol \cdot dm^{-3}$) to 70% (26.3 $mol \cdot dm^{-3}$) leads to a nearly proportional increase of the reaction rate, in agreement with a first-order rate equation. A first order was also reported for MnO_x/Al_2O_3 catalysts.[5,17] In the experimental conditions of our tests, the amount of decomposed H_2O_2 is small compared to the available reagent, thus, H_2O_2 concentration can be assumed constant during each test and equal to the initial concentration n_0/V_{sol}, where n_0 represents mole of H_2O_2 and V_{sol} represents solution volume. The H_2O_2 decomposition rate per catalyst volume, $-(1/V_{cat})(\Delta n/\Delta t)$, after the initial transient, reaches a constant value that is given by

$$-(1/V_{cat})(\Delta n/\Delta t) = k(n_0/V_{sol}) \qquad (2)$$

where V_{cat} represents catalyst volume and k is the kinetic constant.

By means of Eq. (2), kinetic constants are calculated as mean values from tests performed at the same temperatures but with different H_2O_2 concentration and catalyst weights. These values are listed in Table 4. The kinetic constant of MnO_2 is about one order of magnitude higher than those of supported catalysts. However, pure MnO_2, as discussed earlier, has no interest for practical appliances. On the other hand, the activity of Mn/Ti catalysts appear notably high when compared with literature data reported for similar systems: Kinetic constants of 7-Mn/Ti and 10-Mn/Ti catalysts are comparable to or higher than those reported for MnO_2 supported on Al_2O_3 systems.[6]

To obtain information on the intrinsic activity of the supported MnO_2 phase, the molar kinetic constants k', that is, the kinetic constants per mole of MnO_2, (according to EDS analysis), are calculated (Table 4). Note that the increase of MnO_2 content from 5.3 to 7.3% causes an increase of the molar activity, whereas a further increase to 11% produces a slight lowering of molar activity. Thus, there is an optimal MnO_2 content at 7.3%. This could be explained by taking into account that different manganese species are present on the surface of catalysts and that their concentration varies with manganese loading. TPR measurements have shown the presence of Mn species with different oxidation states. It is unlikely that hardly reducible Mn_2O_3 or MnO_2, forming a solid solution with TiO_2, can activate

Table 4 Kinetic constants k and molar kinetic constants k' of MnO_2 and Mn/Ti catalysts

Sample	Temperature, °C	k, $s^{-1} \cdot cm^3_{sol}$ $(cm^3_{cat})^{-1} \times 10^3$	k', $s^{-1} \cdot cm^3_{sol}$ $(mol\ MnO_2)^{-1}$
MnO2	40	39	——
2-Mn/Ti	70	4.7	15.7
5-Mn/Ti	40	1.9	3.1
7-Mn/Ti	40	4.8	5.7
10-Mn/Ti	40	5.6	4.3

a redox mechanism. We can hypothesize that the highly reactive MnO_2 species that are detected in TPR measurements are involved in H_2O_2 decomposition. It has been suggested that the activity of manganese-based catalysts is due to surface Mn^{4+} cations.[7,19] We can hypothesize that H_2O_2 decomposition occurs through the following mechanism involving the redox couple Mn^{4+}/Mn^{3+}:

$$H_2O_2 = HO_2^- + H^+ \quad (3)$$

$$Mn^{4+} + HO_2^- = Mn^{4+}(HO_2)^- \quad (4)$$

$$Mn^{4+}(HO_2)^- \rightarrow Mn^{3+} + HO_{2\cdot} \quad (5)$$

$$HO_{2\cdot} + H_2O_2 \rightarrow OH\cdot + O_2 + H_2O \quad (6)$$

$$Mn^{3+} + OH\cdot \rightarrow Mn^{4+} + OH^- \quad (7)$$

$$H^+ + OH^- = H_2O \quad (8)$$

The first step corresponds to the ionization equilibrium of H_2O_2, which is very fast. Equation (4) represents the adsorption of HO_2^-, also assumed to be very fast and, thus, to exist in pseudoequilibrium conditions. The rate determining step is probably the formation of the radical $HO_{2\cdot}$ [Eq. (5)], in agreement with studies by Salem et al.[21] According to the proposed mechanism, the reaction rate depends at the same time on the kinetics of reduction of Mn^{4+} cations and on their concentration.

The results of TPR characterization are useful to explain the catalytic behavior. It has been observed that the increase of MnO_2 content leads to the formation of more reducible Mn^{4+} oxide species and, at the same time, to lowering of the mean oxidation state of manganese. This gives rise to two opposite effects: The higher reducibility of Mn^{4+} oxide species produces a higher catalytic activity, whereas the formation of less oxidized Mn species (Mn_2O_3) at the expense of MnO_2 causes some lowering of activity. The concurrence of such effects can explain the optimal MnO_2 content corresponding to the maximum intrinsic kinetic rate.

Conclusions

The conclusions of the present work can be summarized as follows:

1) New catalytic systems for H_2O_2 decomposition based on MnO_2 supported on a high surface area TiO_2 are noticeably active when compared with the literature on manganese-based systems.

2) Redox properties of MnO_2 supported on TiO_2 are noticeably modified by interaction with the support, which leads to the formation of MnO_2 species that are more reducible than crystalline MnO_2. Less oxidized and hardly reducible Mn oxides have also been detected.

3) The catalysts show a very high initial activity that does, however, rapidly decrease in time up to the achievement of a stationary value.

4) The intrinsic activity depends on MnO_2 content, and an optimal composition, lower than complete monolayer coverage, has been found.

5) A redox mechanism involving the Mn^{4+}/Mn^{3+} redox couple has been proposed.

Future research should address the definition of preparation procedures and support materials able to stabilize a dispersed MnO_2 phase that avoids the formation of less oxidized phases. Further investigations are also needed to explain the initial transient activity.

References

[1]Mattie, D. R., "Toxicity of Rocket Fuels: Comparison of Hydrogen Peroxide with Current Propellants," *Proceedings of 49th JANNAF Propulsion Meeting*, Vol. 1, Chemical Propulsion Information Agency, Lawer, MD, 1999, pp. 119–122.

[2]Eloirdi, R., Pronier, S., Rossignol, S., Duprez, D., Kappenstein, C., Gibbon, D., Paul, M., Jolley, P., Coxhill, I., and Pillet, N., "An Investigation of Various Catalysts in a Small Hydrogen Peroxide Thruster," *Proceedings of the First International Conference on Green Propellants for Space Propulsion*, Vol. SP-484, ESA, 2001, pp. 173–180.

[3]Pourpoint, T. L., and Rusek, J. J., "Investigation of Homogeneous and Heterogeneous Catalysis for the Propulsive Decomposition of Hydrogen Peroxide," *Proceedings of the First International Conference on Green Propellants for Space Propulsion*, Vol. SP-484, ESA, 2001, pp. 193–197.

[4]Rusek, J. J., "Future of Hydrogen Peroxide for Space Propulsion and Power Applications," *Proceedings of the First International Conference on Green Propellants for Space Propulsion*, Vol. SP-484, ESA, 2001, pp. 1–6.

[5]Pirault-Roy, L., Kappenstein, C., Guerin, M., Eloirdi, R., and Pillet, N., "Hydrogen Peroxide Decomposition on Various Supported Catalysts Effect of Stabilizers," *Journal of Propulsion and Power*, Vol. 18, No. 6, 2002, pp. 1235–1241.

[6]Rusek, J. J., "New Decomposition Catalysts and Characterization Techniques for Rocket-Grade Hydrogen Peroxide," *Journal of Propulsion and Power*, Vol. 12, No. 3, 1996, pp. 574–579.

[7]Hasan, M., Zaki, M. I., Pasupulety, L., and Kumari, K., "Promotion of the Hydrogen Peroxide Decomposition Activity of Manganese Oxide Catalysts," *Applied Catalysis, A: General*, Vol. 181, No. 1, 1999, pp. 171–179.

[8]Zaki, M. I., Hasan, M. A., Paupulety, L., and Kumari, K., "Bulk and Surface Characteristics of Pure and Alkalized Mn_2O_3: TG, IR, XRD, XPS, Specific Adsorption and Redox Catalytic Studies," *New Journal of Chemistry*, 1998, Vol. 22, No. 8, pp. 875–882.

[9]Baral, S., Lume-Pereira, C., Yanata, E., and Henglein, A., "Chemistry of Colloidal Manganese Dioxide. 2. Reaction with Superoxide Anion (O_2^-) and Hydrogen Peroxide (Pulse Radiolysis and Stop Flow Studies)," *Journal of Physical Chemistry*, Vol. 89, No. 26, 1985, pp. 5779–5783.

[10]Zhou, H., Shen, Y. E., Wang, J. Y., Chen, X., O'Young, C. L., and Suib, S. L., "Studies of Decomposition of H_2O_2 over Manganese Oxide Octahedral Molecular Sieve Materials," *Journal of Catalysis*, Vol. 176, No. 2, 1998, pp. 321–328.

[11]Shaheen, W. M., and Selim, M. M., "Effect of Thermal Treatment on Physicochemical Properties of Pure and Mixed Manganese Carbonate and Basic Copper Carbonate," *Thermochimica Acta*, Vol. 322, No. 2, 1998, pp. 117–128.

[12]Radwan, N. R. E., "Surface and Catalytic Properties of Copper Oxide, Manganese Oxide/Silica Systems," *Adsorption Science and Technology*, Vol. 17, No. 7, 1999, pp. 591–610.

[13]Tian, H., Zhang, T., Yang, H., Sun, X., Liang, D., and Lin, L., "Manganese–Lead Mixed Oxide Catalysts for Decomposition of Hydrogen Peroxide," *Cuihua Xuebao*, Vol. 21, No. 6, 2000, pp. 600–602.

[14]Yang, H., Zhang, T., Tian, H., Tang, J., Xu, D., Yang, W., and Lin, L., "Effect of Sr Substitution on Catalytic Activity of $La_{1-x}Sr_xMnO_3$ ($0 \le x \le 0.8$) Perovskite-Type Oxides for Catalytic Decomposition of Hydrogen Peroxide," *Reaction Kinetics and Catalysis Letters*, Vol. 73, No. 2, 2001, pp. 311–316.

[15]Lee, Y. N., Lago, R. M., Fierro, J. L. G., and Gonzalez, J., "Hydrogen Peroxide Decomposition over $Ln_{1-x}A_xMnO_3$ (Ln = La or Nd and A = K or Sr) Perovskites," *Applied Catalysis, A: General*, Vol. 215, No. 1–2, 2001, pp. 245–256.

[16]Yang, H., Zhang, T., Tian, H., Xu, D., Tang, J., and Lin, L., "Decomposition of High Concentration Hydrogen Peroxide over Alumina-Supported $La_{0.6}Sr_{0.4}MnO_3$ Perovskite Catalyst," *Cuihua Xuebao*, Vol. 22, No. 3, 2001, pp. 225–226.

[17]Kappenstein, C., Pirault-Roy, L., Guerin, M., Wahdan, T., Ali, A. A., Al-Sagheer, F. A., and Zaki, M. I., "Monopropellant Decomposition Catalysts. V. Thermal Decomposition and Reduction of Permanganates as Models for the Preparation of Supported MnOx Catalysts," *Applied Catalysis, A: General*, Vol. 234, No. 1–2, 2002, pp. 145–153.

[18]Deraz, N., Allah, M., El-Sayed, M. A., and El-Aal, A. A., "Catalytic Decomposition of H_2O_2 over Manganese Oxides Supported on an Active Alumina," *Adsorption Science and Technology*, Vol. 19, No. 7, 2001, pp. 541–551.

[19]Deraz, N., Allah, M., Salim, H. H., and El-Aal, A. A., "The Influence of Lithium on the Hydrogen Peroxide Decomposition Activity of Manganese-Alumina Catalysts," *Materials Letter*, Vol. 53, No. 1–2, 2002, pp. 102–109.

[20]Shaheen, W. M., Deraz, N. A. M., and Selim, M. M., "Effect of ZnO Doping on Surface and Catalytic Properties of Manganese Oxides Supported on Alumina," Materials Letters, Vol. 52, No. 1–2, 2002, pp. 130–139.

[21]Shaheen, W. M., and Hong, K. S., "Thermal Characterization and Physico-Chemical Properties of Fe_2O_3–Mn_2O_3/Al_2O_3 Systems," *Journal of Thermal Analysis and Calorimetry*, Vol. 68, No. 1, 2002, pp. 289–306.

[22]Salem, I. A., Elhag, R. I., and Khalil, K. M. S., "Catalytic Activity of a Zirconium(IV) Oxide Surface Supported with Transition Metal Ions," *Transition Metal Chemistry*, Vol. 25, No. 3, 2000, pp. 260–264.

[23]Rusek, J. J., and Anderson, N., "Transition Metal Ion-Based High-Activity Monolithic Catalysts for Decomposition of Hydrogen Peroxide in Rocket Engines," U.S. Patent, Application, U.S. 98-45127 19980320, Canadian Patent Application, Docket No. Chemical Abstract Number 134:210171.

[24]Wollner, A., Lange, F., Schmelz, H., and Knözinger, H., "Characterization of Mixed Copper–Manganese Oxides Supported on Titania Catalysts for Selective Oxidation of Ammonia," *Applied Catalysis, A: General*, Vol. 94, No. 2, 1993, pp. 181–203.

[25]Gallardo-Amores, J. M., Armaroli, T., Ramis, G., Finocchio, E., and Busca, G., "A Study of Anatase-Supported Mn Oxide as Catalysts for 2-Propanol Oxidation," *Applied Catalysis B: Environmental*, Vol. 22, No. 4, 1999, pp. 249–259.

[26]Busca, G., Ramis, G., Amores, J. M. G., and Escribano, V. S., "An FT-IR Study of Ammonia Adsorption and Oxidation over Anatase-Supported Metal Oxides," *Applied Catalysis B: Environmental*, Vol. 13, No. 1, 1997, pp. 45–58.

[27]Arnone, S., Busca, G., Lisi, L., Milella, F., Russo, G., and Turco, M., "Catalytic Combustion of Methane over $LaMnO_3$ Perovskite Supported on $La2O_3$ Stabilized Alumina. A Comparative Study with Mn_3O_4, Mn_3O_4–Al_2O_3 Spinel Oxides," *Proceedings of the Twenty-Seventh International Symposium on Combustion*, Combustion Inst., Pittsburgh, PA, 1998, pp. 2293–2299.

[28]Christel, L., Pierre, A., and Rousset Abel, D. A. M., "Temperature Programmed Reduction Studies of Nickel Manganite Spinels," *Thermochimica Acta*, Vol. 306, No. 1–2, 1997, pp. 51–59.

[29]Liu, Y., Luo, M., Wei, Z., Xin, Q., Ying, P., and Li, C., "Catalytic Oxidation of Chlorobenzene on Supported Manganese Catalysts," *Applied Catalysis B: Environmental*, Vol. 29, No. 1, 2001, pp. 61–67.

[30]Villaseñor, J., Reyes, P., and Pecchi, G., "Catalytic and Photocatalytic Ozonation of Phenol on MnO_2 Supported Catalysts," *Catalysis Today*, Vol. 76, No. 2–4, 2002, pp. 121–131.

[31]Laville, F., Gourier, D., Lejus, A. M., and Vivien, D., "Optical and ESR Investigations of Lanthanum Aluminates $LaMg_{1-x}Mn_xAl_{11}O_{19}$ Single Crystals with Magnetoplumbite-Like Structure," *Journal of Solid State Chemistry*, Vol. 49, No. 2, 1983, pp. 180–187.